



The Time-Resolved Magnetic Field Effect in the Spin-Dependent Recombination of Immobile Radical Ion Pairs

Victor A. Bagryansky¹ · Vsevolod I. Borovkov¹ · Yuri N. Molin¹

Received: 13 April 2021 / Revised: 27 May 2021 / Accepted: 9 June 2021 /
Published online: 19 June 2021

© The Author(s), under exclusive licence to Springer-Verlag GmbH Austria, part of Springer Nature 2021

Abstract

The spin evolution of an ensemble of immobile radical ion pairs, assuming different rate constants of the pair recombination in the singlet (k_S) and triplet (k_T) spin states, was investigated for an arbitrary initial state in the absence of paramagnetic relaxation. An analytical solution was obtained for the density matrix of a radical pair at the constant frequency of singlet–triplet transitions. This solution was applied to study how the shape of the curves of the time-resolved magnetic field effect (TR MFE), defined as the ratio of the recombination rates of the pairs in different magnetic fields, depended on the value of $k = k_S - k_T$ in the presence of hyperfine and Zeeman interactions. The former were taken into account using a semi-classical model. It was shown that the shape of TR MFE curves changed dramatically at $k \neq 0$ as compared to the case of $k = 0$. Experimental schemes aimed to reveal the spin-dependent recombination using the TR MFE approach were proposed.

1 Introduction

Spin chemistry methods are successfully used to study radical intermediates of chemical reactions [1]. One of the variants of the related techniques developed is the method of time-resolved magnetic effect (TR MFE) in recombination fluorescence of spin-correlated radical ion pairs (RIPs) [2, 3].

By applying the method, RIPs generated by ionising irradiation of condensed matter are studied. The measured signal is the time-dependent intensity $I(t, B)$ of the radiation-induced recombination fluorescence from the sample as recorded in an external magnetic field B . Typically, the TR MFE curve is determined as the ratio of

✉ Vsevolod I. Borovkov
borovkov@kinetics.nsc.ru

¹ Institute of Chemical Kinetics and Combustion, SB RAS, Institutskaya, 3, 630090 Novosibirsk, Russia

the $I(t, B)$ kinetics at the strong B , i.e., a magnetic field which significantly exceeds the hyperfine interactions in the radicals and zero ($B=0$) magnetic fields

$$TR\ MFE(t) = \frac{I(t, B)}{I(t, 0)} \quad (1)$$

An analysis of this ratio allows one to enhance the effects related to the spin correlation in recombining RIPs against the background of rapidly decaying recombination kinetics. In this way, it is possible to determine the magnetic resonance characteristics of radical ions with their lifetime as short as a few nanoseconds [4]. For radical ions of many organic molecules like alkanes [5] as well as their Group 14 element organometallic [6] or halogenated analogues [7] in solutions, these characteristics have been determined for the first time by using the TR MFE method.

The same approach was also applied to study delayed radiation-induced fluorescence of molecular crystals [8–11] and polymeric systems [12, 13]. If an irradiated medium is composed of luminescent molecules then the main part of the observed luminescence can typically be assigned to an annihilation of triplet excitons. Magnetic field effects in this case originate from the dependence of the spin state evolution of a triplet pair after its first encounter on the external magnetic field [14]. In some cases (see [11–13]), TR MFE observed can be described well assuming that the luminescence appears due to recombination of carriers of electric charge and unpaired electron spin.

The application of the TR MFE method to studies of radical ions in liquids became effective because theoretical models, which allowed extracting with high accuracy the magnetic resonance characteristics of recombining radical ions, were developed. At the same time, the application experience also showed that this method can be implemented properly when a preliminary qualitative analysis of the shape of the TR MFE curves can be performed since this analysis allows one to determine the main interactions affecting the spin evolution of spin-correlated RIPs. An essential assumption of the previously developed theoretical models of TR MFE is that in liquid solution, the efficiency of the recombination of radical ions does not depend on the spin multiplicity of the RIP. To the best of our knowledge, all of the experimental TR MFE curves observed for liquid solutions could be fitted well using this approximation. This indicates that under the conditions of these experiments, the recombination of radical ions with opposite charges in a low-viscosity solution occurs almost immediately at the first diffusion contact, regardless of the RIP spin state.

However, it can be expected that during recombination through tunnelling electron transfer from large distances in solids [15] or high viscosity media, the difference in the formation rate of singlet and triplet reaction products in some cases can be significant due to the different energies of these states.

There were theoretical studies which were previously focussed on taking the spin selectivity in the recombination of radicals in the presence of singlet–triplet transitions into account [16–23]. In the mentioned studies, the problem of the evolution of the RIP spin state with spin selective radical recombination was solved or, at least, a way to obtain such a solution was described. In these studies, different approaches

were used and, mainly, the goal was to analyse the effect of a magnetic field on the yield of radical recombination products.

In the present work, we have proposed and used another way to find an analytical solution of the problem. The approach, which is based on reducing the evolution operator to a fairly simple form, was applied to calculate the TR MFE curves taking into account Zeeman as well as hyperfine interactions and to discuss the qualitative manifestations of spin selectivity in the RIP recombination in the TR MFE curves.

2 Theoretical Backgrounds

Consider an ensemble of radical pairs AB with time-independent rate constants from the singlet state k_S and the triplet states k_T . This case corresponds, in particular, to a RIP created in a covalently linked dyad with a fixed distance between partners immobilised in a matrix and to the recombination through a tunnelling. In the presence of a spin-selective recombination reaction, the equation for the density matrix $\rho(t)$ has the following form [24]:

$$\begin{aligned}\dot{\rho} &= -i[H, \rho] - \frac{k_S}{2}(P_S\rho + \rho P_S) - \frac{k_T}{2}[(1 - P_S)\rho + \rho(1 - P_S)] \\ &= -i[H, \rho] - \frac{k_S - k_T}{2}(P_S\rho + \rho P_S) - k_T\rho,\end{aligned}\quad (2)$$

where H is the Hamiltonian and P_S is the operator of the projection onto the singlet state of RIP, which is equal to:

$$P_S = \frac{1}{4} - \vec{a} \cdot \vec{b}, \quad (3)$$

where \vec{a} and \vec{b} are vectors composed of the operators of the projections of the electron spins of the radicals A and B .

In the present work, neither dipole–dipole interactions within the RIP nor its paramagnetic relaxation were included in the consideration since this simplification allowed us to obtain an analytical solution. At the same time, this approximation is correct if the RIP's partners are separated by a distance long enough that hyperfine interaction (HFI) exceeds the dipole–dipole interaction. As for paramagnetic relaxation, it can be anticipated that in a solid matrix for an isolated organic radicals, the relaxation is much slower as compared to the singlet–triplet mixing due to HFI. Below, radiation-generated RIPs with a wide spatial distribution are also discussed. For such RIPs, this approximation seems to be useful when the RIP recombination is rapid enough that closely spaced RIPs decays before both HFI and dipole–dipole interactions become important.

The solution to Eq. (2) is:

$$\rho(t) = \exp(-k_T t) \exp\left[\left(-\frac{k}{2}P_S - iH\right)t\right] \rho(0) \exp\left[\left(-\frac{k}{2}P_S + iH\right)t\right] = \exp(-k_T t) \Pi^* \rho(0) \Pi, \quad (4)$$

where $k = k_S - k_T$, $\Pi = \exp \left[\left(-\frac{k}{2} P_S + iH \right) t \right]$. In the absence of interaction between the electron spins of radicals A and B in a strong magnetic field the Hamiltonian has the form:

$$H = \omega_a a_Z + \omega_b b_Z. \quad (5)$$

In the absence of hyperfine interaction (HFI), the quantities $\omega_{a,b}$ are the frequencies of the Larmor precession of electron spins $\omega_{a,b} = \omega_{0a,b}$. In the presence of an isotropic HFI in a strong magnetic field, for RIP sub-ensembles with certain values of the projections of nuclear spins, one should set $\omega_{a,b} = \omega_{0a,b} + \sum m_{a,b} \alpha_{a,b}$, where $\alpha_{a,b}$ are isotropic constants of HFI and $m_{a,b}$ are the projections of nuclear spins on the fields direction, the summation is performed over the magnetic nuclei. To obtain a solution for the full ensemble, these solutions should be averaged over the distribution of the $m_{a,b}$ projection sets.

As follows from Eqs. (3), (4) and (5), the operators Π and Π^* are functions of the operators of the projections of the spins $1/2$, any function of which can be represented as a linear function [25]. To produce such a representation, we used the existing analytical solutions [26] for the eigenfunctions and eigenvalues of the operators $\left(-\frac{k}{2} P_S \pm iH \right)$, which are in the exponents of the exponential operators Π and Π^* . Calculating the result of the action of the operators Π and Π^* on these eigenfunctions, we obtain a system of linear equations, the solution of which has the following form:

$$\Pi = P + Q\vec{a} \cdot \vec{b} + Ra_Z + Sb_Z + Ta_Zb_Z, \quad (6)$$

where

$$P = \frac{1}{2} \left(c_+ + e^{-\frac{kt}{4}} \cos(pt) \right), \quad (7)$$

$$Q = e^{-\frac{kt}{4}} \frac{k}{2p} \sin(pt), \quad (8)$$

$$R = i \left(s_+ + e^{-\frac{kt}{4}} \frac{\Omega}{2p} \sin(pt) \right), \quad (9)$$

$$S = i \left(s_+ - e^{-\frac{kt}{4}} \frac{\Omega}{2p} \sin(pt) \right), \quad (10)$$

$$T = 2 \left[c_+ - e^{-\frac{kt}{4}} \left(\cos(pt) + \frac{k}{4p} \sin(pt) \right) \right], \quad (11)$$

$$c_+ = \cos \left(\frac{\omega_a + \omega_b}{2} t \right), s_+ = \sin \left(\frac{\omega_a + \omega_b}{2} t \right), \Omega = \omega_a - \omega_b, p = \frac{1}{4} \sqrt{4\Omega^2 - k^2}. \quad (12)$$

Using Eq. (4) and Eqs. (6)–(12), we can express $\rho(t)$ for any initial data $\rho(0)$ as a linear function of the operators of the projections of spins a_i and b_j and their products $a_i b_j$ with coefficients depending on time and parameters ω_a, ω_b , and k .

3 Population of the Singlet State

As the TR MFE method is based on the observation of recombination fluorescence, to simulate the results obtained by this method, it is necessary to calculate the population of the singlet state of a RIP ensemble:

$$\rho_S(t) = Tr[P_S \rho(t)], \tag{13}$$

where Tr denotes the trace of operator.

Suppose that in the initial state the fraction of pairs in the singlet state is equal to θ , and the remaining RPs with the fraction $(1 - \theta)$ are in a random spin state. In this case:

$$\rho(0) = \left(\frac{1}{4} - \vec{a} \cdot \vec{b}\right)\theta + \frac{1}{4}(1 - \theta) = \frac{1}{4} - \theta \vec{a} \cdot \vec{b}. \tag{14}$$

At $\theta = 1$ this is the singlet state of the entire ensemble. At $\theta = 0$ all four spin states are uniformly populated. At $\theta = -1/3$, the initial state Eq. (14) corresponds to uniform population of three triplet states at zero population of the singlet state.

Using Eqs. (3), (6)–(13), we obtain the following result for the population of the singlet state:

$$\begin{aligned} \rho_{\theta S}(t) = & \frac{1}{4} \exp(-k_T t) \exp\left(-\frac{kt}{2}\right) \\ & \times \left[(1 + 3\theta) \left(\cos(pt) - \frac{k}{4p} \sin(pt) \right)^2 + (1 - \theta) \frac{\Omega^2}{4p^2} \sin^2(pt) \right]. \end{aligned} \tag{15}$$

Note that although Eq. (7) and Eqs. (9)–(11) are dependent on the sum of frequencies $\omega_a + \omega_b$, Eq. (15) includes only their difference Ω . For $k < 2|\Omega|$, Eq. (15) has the form of oscillations with a frequency $2p < |\Omega|$. The oscillations are shifted in phase and decay in time and both the shift and the decay rate increase with increasing the value of k (Fig. 1). For $k > 2|\Omega|$, Eq. (15) becomes non-oscillating (Fig. S1 in Supplementary Material 1).

It is worth noting that for $\theta = 1$, Eq. (15) coincides up to a constant with the time dependent evolution of a two-level quantum system in the presence of Rabi oscillations between the two levels with frequency Ω and continuous partial measurement [27] if the value of k in Eq. (15) is given the meaning of the measurement strength parameter. This may be relevant to the discussion on the choice of the reaction superoperator form (see, for example, [28] and references therein).

Figure 1 shows the time dependences of the population of the singlet state Eq. (15) for $k = \Omega/3, k_T = 0$ and different values of θ . It can be seen that in all cases,

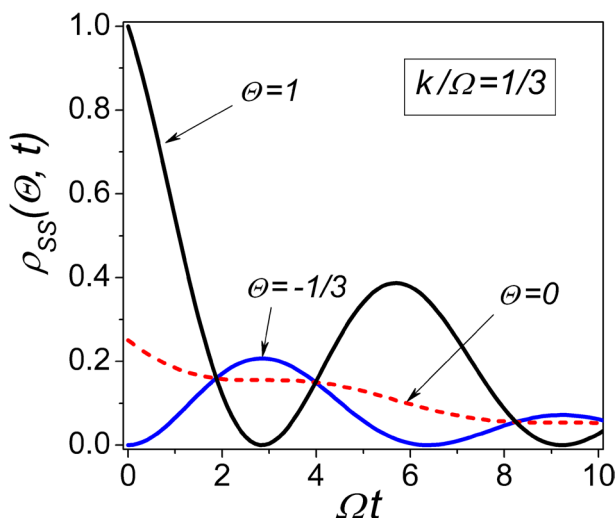


Fig. 1 Time dependent population of the singlet spin state of RIP ensemble at $k = \Omega/3$, $k_T = 0$ and $\theta = 1$, $\theta = 0$ (dashed line), $\theta = -1/3$ as indicated in the plot

even with the initial equiprobable population of all spin states with $\theta = 0$, decaying oscillations in the population of the singlet state with time is observed. All of the curves, corresponding to different θ values, intersect at some times, t^* , which are determined by the condition of equality to zero of the time-dependent coefficient at the factor θ in Eq. (15) and obey the relation $\tan(p t^*) = \frac{4\sqrt{3}p}{\sqrt{3k \pm 2\Omega}}$. Similar moments in time, in which the population does not depend on the initial spin state, exist for non-oscillating solutions, too (Fig. S1 in Supplementary Material 1).

4 TR MFE in the Semi-classical Approximation for HFI in One of the RIP Partners

As already noted, the experimentally determined TR MFE curve is equal to the ratio (1) of the kinetics of recombination fluorescence in strong and zero magnetic fields. In the recombination model that we used, a short fluorescence time of the recombination product in the singlet state results in the fluorescence kinetics determined by the product $k_S \rho_{\theta S}(t)$. This means that TR MFE is equal to the ratio of the time-dependent populations of the singlet state in strong and zero magnetic fields:

$$TR\ MFE = \frac{k_S \rho_{\theta S}(t, B)}{k_S \rho_{\theta S}(t, 0)} = \frac{\rho_{\theta S}(t, B)}{\rho_{\theta S}(t, 0)}. \quad (16)$$

Solution Eq. (15) makes it possible to calculate the value of $\rho_{\theta S}(t, B)$ in a strong field for any HFI in each of the radicals. At zero magnetic field, the value of $\rho_{\theta S}(t, 0)$ and, consequently, TR MFE curve Eq. (16) can also be calculated using Eq. (15) in the semi-classical Schulten–Wolynes approximation [29] for HFI in one of the

radicals and in the absence of HFI in its partner. In this approximation, the HFI with magnetic nuclei is replaced by an effective magnetic field with a Gaussian distribution of the probabilities of the values of its projections on a coordinate axis if the number of magnetic nuclei is sufficiently large.

Assuming that the rate constants k_S and k_T do not depend on the magnetic field, the population of the singlet state in a strong field can be calculated by averaging over projection of the effective magnetic field on external magnetic field as follows:

$$\frac{1}{\sigma\sqrt{2\pi}} \int_{-\infty}^{\infty} e^{-\frac{x^2}{2\sigma^2}} \left[(1 + 3\theta) \left(\cos(pt) - \frac{k}{4p} \sin(pt) \right)^2 + (1 - \theta) \frac{\Omega^2}{4p^2} \sin^2(pt) \right] dx, \quad (17)$$

where $\Omega = \omega_{0a} + x - \omega_{0b}$, σ^2 is the mean square of the magnetic moment of nuclei, expressed in frequency units. The value of σ^2 can be easily calculated for any set of nuclear spins and HFI with them, as in the case of both isotropic [29] and, with a random orientation of the principal axes of the HFI tensors, anisotropic [11] interactions. Note that the σ value can be used as a scale for other interactions.

For a zero field, it is required to calculate the integral for $\Omega = x$ over random orientations of the HFI-related effective magnetic field in three-dimensional space that can be performed as follows:

$$\frac{\sqrt{2}}{\sigma^3\sqrt{\pi}} \int_0^{\infty} x^2 e^{-\frac{x^2}{2\sigma^2}} \left[(1 + 3\theta) \left(\cos(pt) - \frac{k}{4p} \sin(pt) \right)^2 + (1 - \theta) \frac{\Omega^2}{4p^2} \sin^2(pt) \right] dx. \quad (18)$$

Note that within the framework of this model, TR MFE is determined precisely by the ratio of integrals Eqs. (17) and (18).

5 Recombination at $k = \text{const}$

Consider an ensemble of RIPS having the same k value that, for example, corresponds to radical centres which are covalently linked by a rigid spacer. Figure 2 shows the results of a numerical calculation of the TR MFE curves determined by Eqs. (16)–(18) at $\theta = 1$ and the same g -factors of the RIP partners, $\omega_{0a} - \omega_{0b} = 0$. The varied parameter was the ratio k/σ .

The upper TR MFE curve corresponds to $k = 0$, which is the case of the equal rate constants of recombination from the singlet and triplet states $k_S = k_T$. This curve has a maximum which is located at time $t \approx 1.6/\sigma$ and followed by a monotonic decay to unity. It should be noted that in the study of radical ions with the unresolved EPR spectra in solution [2, 3], the second moment of the distribution by HFI constants was determined based on the position of this peak. As the difference $k = k_S - k_T$ increases, the maximum shifts to shorter times. After the peak, the MFE curve falls to values significantly less than unity and then rises at large times (see Fig. S2 in Supplementary Material 1). The rate of this rise varies non-monotonically with k and the growth proceeds at a maximum rate at values of $k \approx 2\sigma$.

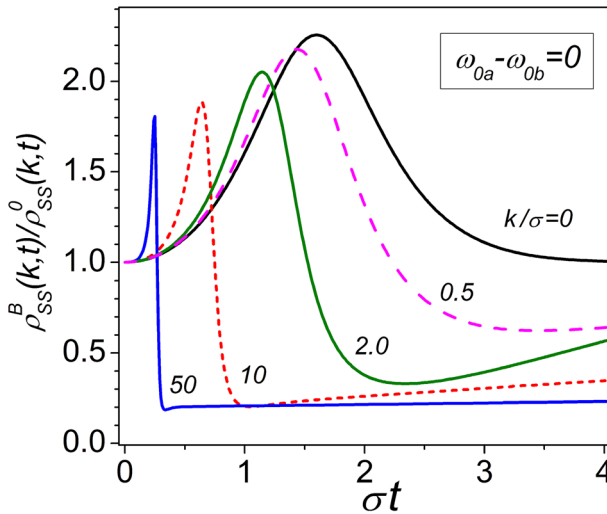


Fig. 2 Dependences of the ratio Eq. (16) of the RIP singlet state populations at strong and zero magnetic fields on time at $\theta=1$, $\omega_{0a}-\omega_{0b}=0$ and different values of the k/σ ratio (0; 0.5; 2; 10; 50) as indicated in the plot

Though the integrals Eqs. (17) and (18), generally, can only be calculated numerically, the linear growth of the TR MFE curves in time at $k/\sigma \gg 1$ can also be revealed by simplifying the integrands. As mentioned above, under the inequality $k > 2|\Omega|$, Eq. (15) has a decaying non-oscillating character. In this case, Eq. (15) can be represented as the sum of three terms which decay exponentially to zero. When calculating Eqs. (17) and (18) at large times, it is sufficient to take into account only that term which decays most slowly. At $\theta=1$, this term is proportional to $\exp(-x^2 t/k)$. This dependence on x makes it possible, together with the expansion of the corresponding coefficient in terms of the small parameter $x^2 t/k$, to carry out the integration analytically and to obtain for appropriate t :

$$MFE \rightarrow \frac{1}{5} + \frac{2\sigma^2 t}{5k}. \quad (19)$$

The trial calculations have shown that this limiting ratio describes well the long-time behaviour of the TR MFE curves already at $k/\sigma > 5$ (see Fig. S3 in Supplementary Material 1). Note that a similar long-time increase can be found at other values of θ , too (Figs. S4 and S5 in Supplementary Material 1).

Again, at $k \gg \sigma$, an analytical estimation is possible for the time t_{\max} , which corresponds to the position of the TR MFE maximum. Consider, for example, the case of $\theta=1$. If we assume that the indicated maximum of TR MFE is reached approximately at the moment when expression Eq. (18) reaches the minimum, then, expanding Eq. (18) in series of the small parameter σ/k , we can obtain $t_{\max} \approx \frac{1}{k} \ln\left(\frac{k^4}{15\sigma^4}\right)$. Comparison with numerical calculations shows that this estimate is valid with an accuracy of about 15% at $k/\sigma \geq 5$ (see Figure S6 in

Supplementary Material 1). In a similar way, it can be shown that the amplitude of the discussed peak decreases with increasing k to a value of about 1.5. Thus, at $k/\sigma \gg 1$, the position of the peak is primarily determined by the difference in the rate constants of recombination of pairs of different multiplicity. The above estimates can be useful for a qualitative interpretation of experiments in which the reaction rate varies with temperature.

The influence of the difference in the g -factors on the form of the TR MFE curves is illustrated with Fig. 3, which shows the curves for the values $\theta = 1$ and $k/\sigma = 10$ and for different values of $\omega_{0a} - \omega_{0b}$ assuming further that $\omega_{0a} > \omega_{0b}$. At values $(\omega_{0a} - \omega_{0b})/\sigma < 1$, the difference in the frequencies of the Larmor precession of the radicals has little effect on both the amplitude and position of the maximum in the TR MFE curve. In the range of values $(\omega_{0a} - \omega_{0b})/\sigma > 1$, this maximum shifts somewhat towards longer times. As the analysis of approximate solutions at $k \gg (\omega_{0a} - \omega_{0b})$ showed, for $(\omega_{0a} - \omega_{0b})/\sigma > 2$ the magnitude of the shift is about $\Delta t \approx \frac{\ln(4)}{k}$. In this case, the peak amplitude increases with a further increase in $(\omega_{0a} - \omega_{0b})$ as $(\omega_{0a} - \omega_{0b})^4$. The appearance of oscillations at times before the maximum of the TR MFE curve, i.e., so-called Δg -beats [2, 3], becomes noticeable only in the opposite limiting case $k \ll (\omega_{0a} - \omega_{0b})$. The behaviour of the “tails” of the MFE curves also changes significantly. The growth of the MFE curves with time disappears, and they all remain localised in the region $MFE < 1$ (Fig. S7 in Supplementary Material 1).

Therefore, this consideration shows that there is a dramatic difference in the manifestation of the difference in the frequencies of the Larmor precession of radicals in the TR MFE curves under the condition $k > 0$ as compared to the previously

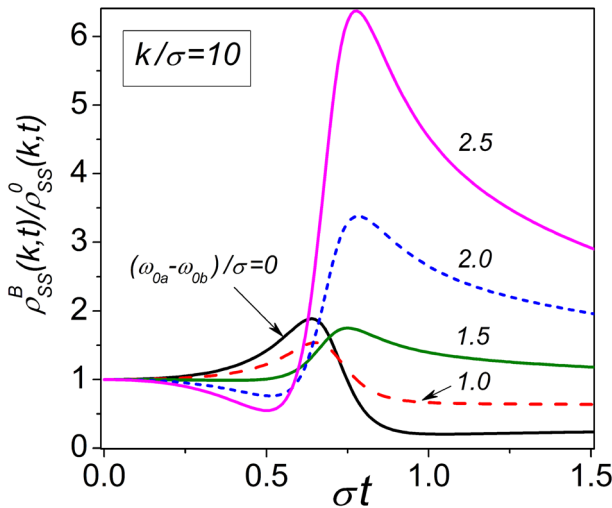


Fig. 3 Dependences of the ratio Eq. (16) of the RIP singlet state populations at strong and zero magnetic fields on time at $\theta = 1$, $k/\sigma = 10$ at the different values of the $(\omega_{0a} - \omega_{0b})/\sigma$ ratio (0; 1; 1.5; 2; 2.5) as indicated in the plot

observed Δg -beats in solutions [2, 3]. Since in the experiment it is easy to vary the value of $(\omega_{0a} - \omega_{0b})$ by changing the external magnetic field, the discussed dependence can serve as a tool for distinction and studies of the spin-dependent recombination.

6 Pairs With Distribution Over k Values

Frequently, in studies of radical ions in the solid phase, RIPs are generated using high-energy irradiation of the sample. In this case, the pairs are separated by different distances, due to which the recombination rate for different pairs can differ significantly. Let us consider the features of the TR MFE curves in a rather simplified situation. Assume that $k_T = 0$ and $k = k_S$, which depends on the distance r between radicals as $k(r) = k_0 \cdot \exp(-r/a)$, where k_0 is the rate constant of the recombination of the radicals at their contact, which is a typical assumption for tunnelling recombination [15]. We also use the exponential distribution function over the distances between radicals $f(r) = 1/b \cdot \exp(-r/b)$ so, in this case, TR MFE depends only on the ratio, a/b , of these distribution parameters.

TR MFE curves were calculated numerically by averaging the quantities $k(r) \cdot \rho_{\theta S}(t, r)$ over the values of r for a strong and zero fields and by calculating the values $\rho_{\theta S}(t, r)$ in the semi-classical approximation. In Figs. 4 and 5, the results of such calculations are compared with the curves calculated in the case of $k = \text{const}$. In the calculations, we set $a/b = 0.04$ based on the typical values of these parameters, $b \sim 5$ nm and $a \sim 0.2$ nm [15]. It is worth noting that calculations have shown that

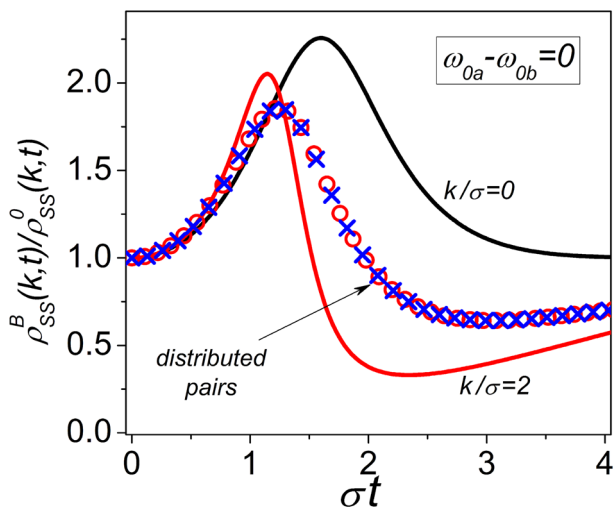


Fig. 4 Dependences of the ratio Eq. (16) of the RIP singlet state populations at strong and zero magnetic fields on time at the fixed values of k/σ (solid lines) and the same for the pairs distributed over radical–radical distances r as $f(r) = 1/b \exp(-r/b)$ for the rate constant distance dependence of $k(r) = k_0 \cdot \exp(-r/a)$ at $a/b = 0.04$, $k_0/\sigma = 10^2$ (circles) and $k_0/\sigma = 10^4$ (crosses), $\theta = 1$. The g -factors of the RIP partners are the same, calculation parameters are given in the plot

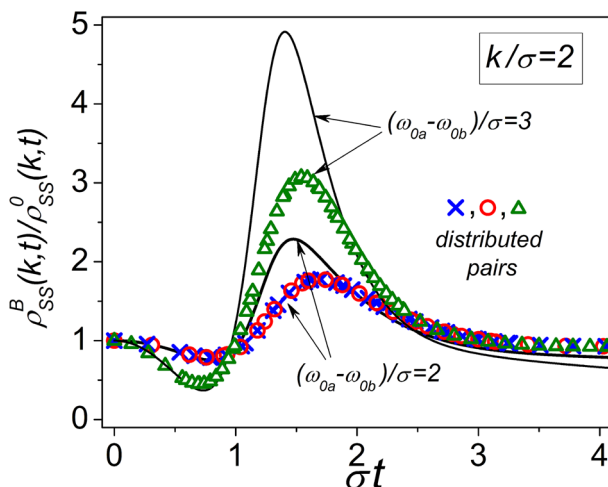


Fig. 5 Dependences of the ratio Eq. (16) of the RIP singlet state populations at strong and zero magnetic fields on time at the fixed value of $k/\sigma=2$ (solid lines) and the same for the pairs distributed over radical–radical distances r as $f(r)=1/b \exp(-r/b)$ for the rate constant distance dependence of $k(r)=k_0 \exp(-r/a)$ at $a/b=0.04$, $k_0/\sigma=10^2$ (circles, triangles) and $k_0/\sigma=10^4$ (crosses), $\theta=1$. The values of the $(\omega_{0a} - \omega_{0b})/\sigma$ ratio for the RIP partners are given in the plot

varying the a/b ratio over a wide range has little effect on the shape of the TR MFE curves.

According to the calculations, the difference in the rate constants of recombination of pairs of different multiplicity, k , becomes unimportant for TR MFE curves in the presence of a wide distribution of radical pairs (Fig. 4), though the recombination kinetics is strongly affected by this distribution. In contrast to the curves shown in Fig. 2, varying the value of the pre-exponential factor k_0 by the orders of magnitude does not change these curves noticeably.

Instead, the maximum position of the TR MFE curve always corresponds nearly to $k/\sigma=2$ in the case of a fixed value of k (Fig. 4). This can be explained by the fact that with an increase in k_0 , the characteristic distance, which separates the main part of the pairs recombining at a given moment, also increases [15]. Thus, due to the strong exponential decay of $k(r)$, the rate of pair recombination at this moment changes much less than the value of k_0 itself. The effect of the very weak influence of the corresponding pre-exponential factor on the kinetics of tunnelling recombination was also observed under more realistic conditions of the radiation experiment, when recombination occurs in spurs, including several closely spaced pairs [13].

On the other hand, the manifestation of difference in the g -factors of recombining radicals in the shape of TR MFE curves remains qualitatively the same on going from $k=\text{const}$ to a wide distribution over $k(r)$ (Fig. 5). This indicates that the analysis of the field dependence of TR MFE makes it possible to reveal the dependence of the recombination rate constant on the spin state of pairs, even under conditions of insufficient information on the track structure and on the details of the spatial distribution of radical pairs over distances.

Although the problem of constructing an analytical model at low or zero magnetic fields has limited our consideration to the case of an unresolved EPR spectrum in one partner only, the proposed model can be used to analyse an arbitrary set of HFI constants in spin-correlated RIPs. For example, when studying radical pairs with HFI and a nonzero difference in the g -factors, one can compare the kinetics recorded in different magnetic fields which both significantly exceed HFI and, at the same time, differ significantly from each other. In this case, Eq. (15) is applicable for an arbitrary EPR spectrum. An analysis of the TR MFE curves can generally provide information on HFI in both radicals. A similar experimental scheme was previously used in studies of the so-called Δg -beats in the recombination fluorescence of spin-correlated radical ion pairs [30].

7 Conclusion

In this work, we addressed the problem of calculating the time-resolved magnetic field effect in the tunnelling recombination of immobile radical ion pairs with the dependence of the recombination rate constant on the spin state of the pair. The solution to this problem can be applied, in particular, for the analysis of TR MFE in polymer systems and low-temperature glasses. Our efforts were aimed at obtaining an analytical solution that would make it possible to carry out a qualitative analysis of the shape of the TR MFE curves and thus reveal the main interactions which determine the evolution of the spin state of an ensemble of radical pairs.

Using a semi-classical model to take into account hyperfine interactions in one of the radicals of a pair, the dependence of the shape of the TR MFE curves on various parameters and the distance distribution of the pairs were analysed. It was found that the difference in the rates of recombination from singlet and triplet states greatly changes the shape of TR MFE curves in comparison with the previously studied case of recombination in solutions. To reveal experimentally the dependence of the rate constant of tunnelling recombination on the spin state of the recombining pairs, various experimental schemes were proposed.

Supplementary Information The online version contains supplementary material available at <https://doi.org/10.1007/s00723-021-01368-5>.

Funding YuNM is grateful to the Russian Science Foundation (Project No. 20-63-46034) for financial support.

Data Availability Not applicable.

Code Availability Not applicable.

Declarations

Conflict of interest The authors declare no conflicts of interest.

References

1. K.M. Salikhov, Y.N. Molin, R.Z. Sagdeev, A.L. Buchachenko, *Spin Polarization and Magnetic Effects in Radical Reactions* (Elsevier, Amsterdam, 1984)
2. V. Borovkov, D. Stass, V. Bagryansky, Y. Molin, in *Applications of EPR in Radiation Research*, ed. by A. Lund, M. Shiotani (Springer International Publishing, Cham, 2014), p. 629
3. V.A. Bagryansky, V.I. Borovkov, Y.N. Molin, *Russ. Chem. Rev.* **76**, 493 (2007)
4. V.I. Borovkov, I.V. Beregovaya, L.N. Shchegoleva, S.V. Blinkova, D.A. Ovchinnikov, LYu. Gurskaya, V.D. Shteingarts, V.A. Bagryansky, Y.N. Molin, *J. Phys. Chem. A* **119**, 8443 (2015)
5. P.A. Potashov, V.I. Borovkov, L.N. Shchegoleva, N.P. Gritsan, V.A. Bagryansky, Y.N. Molin, *J. Phys. Chem. A* **116**, 3110 (2012)
6. V.I. Borovkov, V.A. Bagryansky, Yu.N. Molin, M.P. Egorov, O.M. Nefedov, *Phys. Chem. Chem. Phys.* **5**, 2027 (2003)
7. V.I. Borovkov, *J. Phys. Chem. B* **122**, 8750 (2018)
8. M. Binder, C.E. Swenberg, N.E. Geacintov, *Phys Status Solidi B* **97**, K21 (1980)
9. C. Fuchs, J. Klein, R. Voltz, *Radiat. Phys. Chem.* (1977) **21**, 67 (1983)
10. G.J. Baker, B. Brocklehurst, I.R. Holton, *J. Phys. B At. Mol. Phys.* **20**, L305 (1987)
11. V.I. Borovkov, V.A. Bagryansky, G.A. Letyagin, I.V. Beregovaya, L.N. Shchegoleva, Y.N. Molin, *Chem. Phys. Letters* **712**, 208 (2018)
12. V.I. Borovkov, L.N. Shchegoleva, *J. Phys. Chem. C* **123**, 28058 (2019)
13. V.I. Borovkov, A.I. Taratayko, Y.N. Molin, *J. Phys. Chem. B* **123**, 5916 (2019)
14. U.E. Steiner, T. Ulrich, *Chem. Rev.* **89**, 51 (1989)
15. R.F. Khairutdinov, K.I. Zamaraev, V.P. Zhadanov, *Electron Tunneling in Chemistry. Chemical Reactions over Large Distances* (Elsevier Science, Amsterdam, 1989)
16. K. Schulten, H. Staerk, A. Weller, H.-J. Werner, B. Nickel, *Z. Phys. Chem.* **101**, 371 (1976)
17. U. Till, P.J. Hore, *Mol. Phys.* **90**, 289 (1997)
18. A.B. Doktorov, J.B. Pedersen, *Chem. Phys. Letters* **423**, 208 (2006)
19. A.B. Doktorov, J.B. Pedersen, *Chem. Phys.* **322**, 433 (2006)
20. A.M. Lewis, D.E. Manolopoulos, P.J. Hore, *J. Chem. Phys.* **141**, 044111 (2014)
21. T.P. Fay, L.P. Lindoy, D.E. Manolopoulos, *J. Chem. Phys.* **149**, 064107 (2018)
22. V.L. Berdinskii, I.N. Yakunin, *Dokl. Phys. Chem.* **421**, 163 (2008)
23. I.N. Yakunin, V.L. Berdinskii, *Russ. J. Phys. Chem. B* **4**, 384 (2010)
24. R. Haberkorn, *Mol. Phys.* **32**, 1491 (1976)
25. L.D. Landau, L.M. Lifshitz, *Quantum Mechanics: Non-Relativistic Theory*, 3rd edn. (Pergamon Press, 2013), pp. 197–224
26. I.N. Yakunin, V.L. Berdinskii, *Russ. J. Phys. Chem. B* **4**, 210 (2010)
27. P. Kumar, A. Romito, K. Snizhko, *Phys. Rev. Res.* **2**, 043420 (2020)
28. R.H. Keens, D.R. Kattnig, *New J. Phys.* **22**, 083064 (2020)
29. K. Schulten, P.G. Wolynes, *J. Chem. Phys.* **68**, 3292 (1978)
30. A.V. Veselov, V.I. Melekhov, O.A. Anisimov, Yu.N. Molin, *Chem. Phys. Letters* **136**, 263 (1987)

Publisher's Note Springer Nature remains neutral with regard to jurisdictional claims in published maps and institutional affiliations.